

**Synthesis and Applications of Graphite Carbon Sphere with Uniformly  
Distributed Magnetic Fe<sub>3</sub>O<sub>4</sub> Nanoparticles (MGCSs) and MGCS@Ag,  
MGCS@TiO<sub>2</sub>**

*Yang Liu<sup>a</sup>, Zhiyu Ren<sup>a</sup>, Yuanlong Wei<sup>b</sup>, Baojiang Jiang<sup>a</sup>, Shanshan Feng<sup>a</sup>, Lingyi  
Zhang<sup>b</sup>, Weibing Zhang<sup>b\*</sup> and Honggang Fu<sup>a\*</sup>*

<sup>a</sup> Key Laboratory of Functional Inorganic Material Chemistry, Ministry of Education  
of the People's Republic of China, Heilongjiang University, Harbin 150080 P. R.  
China

E-mail: fuhg@vip.sina.com

Tel.: +86 451-86608458; Fax: +86 451-86673647

<sup>b</sup> School of Chemistry and Molecular Engineering, East China University of Science  
and Technology, Shanghai 200237 P. R. China

E-mail: weibingzhang@ecust.edu.cn

Tel.: +86 21-64252145; Fax: +86 21-64233161

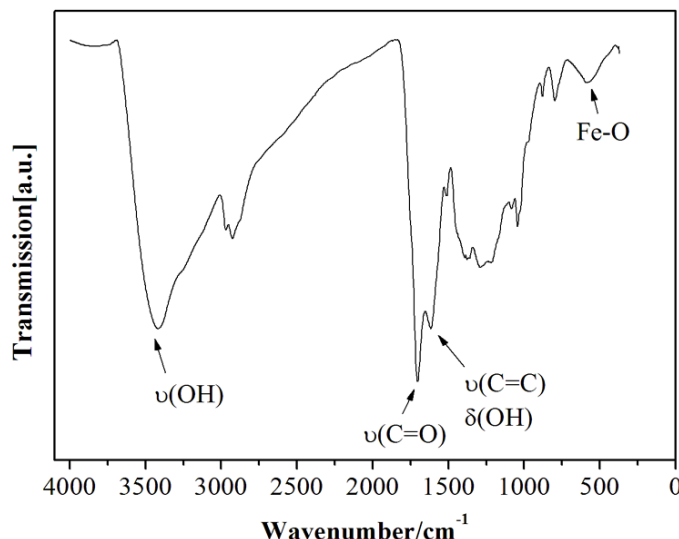
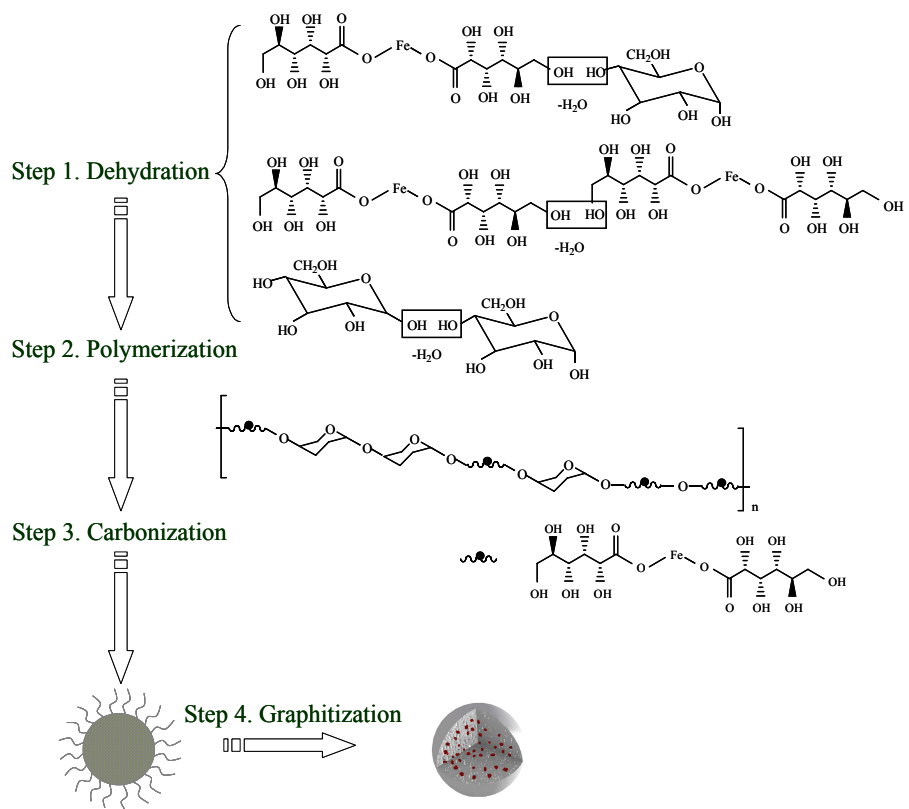


**Fig. S1** FT-IR spectra of CCSs prepared by synchronously hydrothermal reaction of glucose and ferrous gluconate.



**Scheme S1** Schematic illustration of formation mechanism of CCSs and MGCSs.

The detailed structure of CCSs can be observed by TEM. There are no nanoparticles in the TEM image of the triturated CCSs (Fig. S2(A)), which implies that Fe(II) don't convert to iron oxide particles during the synchronous hydrothermal reaction. This is also verified by XRD pattern of CCSs (Fig. 2A(a)). Meanwhile, the distribution of Fe(II) can be verified by the XEDS elemental mapping of Fe and C from the TEM image of the triturated CCSs. These results imply that the Fe(II) can be enwrapped in the carbonaceous matrix uniformly.

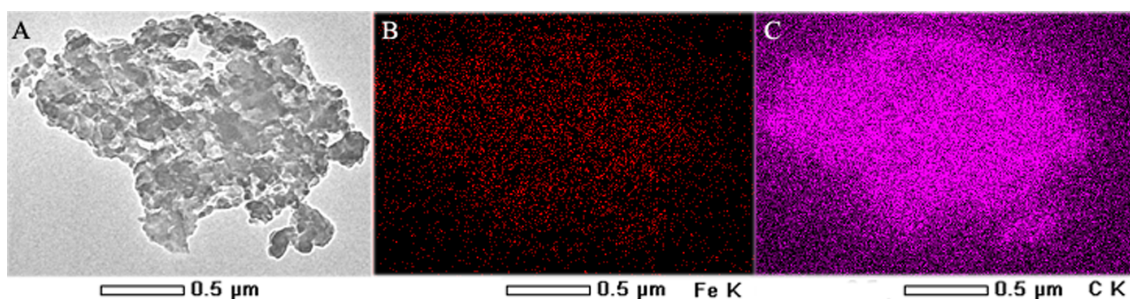


**Fig. S2** (A) TEM image of the triturated CCSs; (B, C) XEDS elemental mapping of Fe and C from the image in (A).

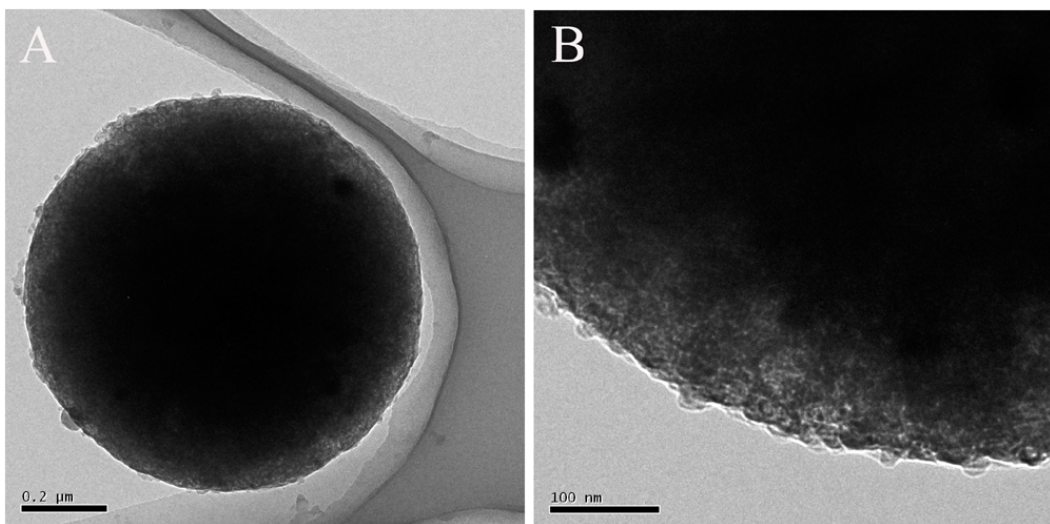


**Fig. S3** Typical TEM images of MGCSs: (A) individual graphite sphere; (B) a detailed view of the edge of graphite sphere.

Fe(II) in CCSs change to magnetic Fe<sub>3</sub>O<sub>4</sub> nanoparticles during high temperature carbonization under N<sub>2</sub> protection, which have been revealed by XRD patterns of CCSs and MGCSs (Fig. 2A). The conversion maybe attribute to the produced carbon dioxide during the decomposition of organic gluconate and glucose. Here, TG coupled to a FT-IR (TG/FT-IR) technique was used to certify the oxidation effect of carbon dioxide (Fig. S4). Compared with the evolution of the IR spectra in the region 2200-2000 cm<sup>-1</sup> (CO) and 2300-2500 (CO<sub>2</sub>) cm<sup>-1</sup>, the bands of CO gas appear with the weakening of the bands of CO<sub>2</sub> gas when the temperature increase to 600 °C. This result illuminates that the part of CO<sub>2</sub> gas were reduced to CO gas, which indicate the CO<sub>2</sub> gas could use as the oxidant to cause the forming of Fe<sub>3</sub>O<sub>4</sub> nanoparticles. In addition, the conversion of Fe(II) to iron oxide was also observed via the direct pyrolysis of ferrous gluconate under N<sub>2</sub> protection (Ref 22 in the paper).

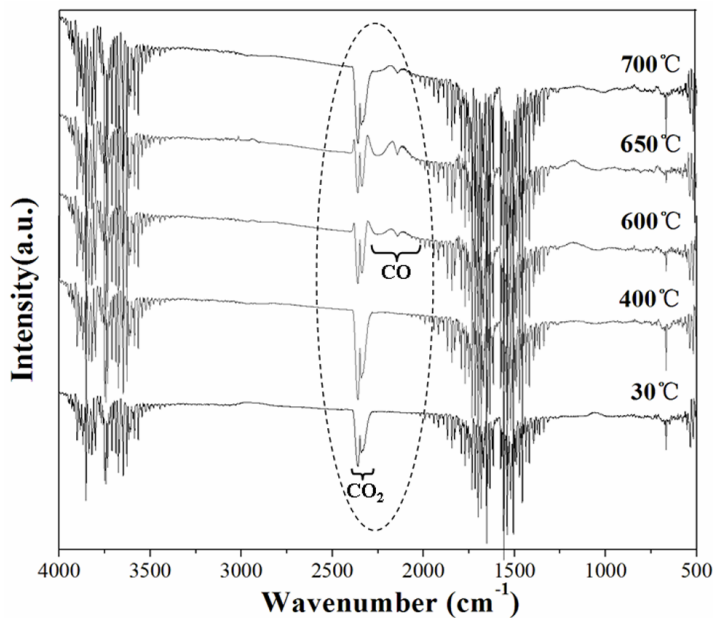


**Fig. S4** Evolution with the temperature of the FT-IR spectra of the gases evolved in the thermal pyrolysis of CCSs under N<sub>2</sub> protection.

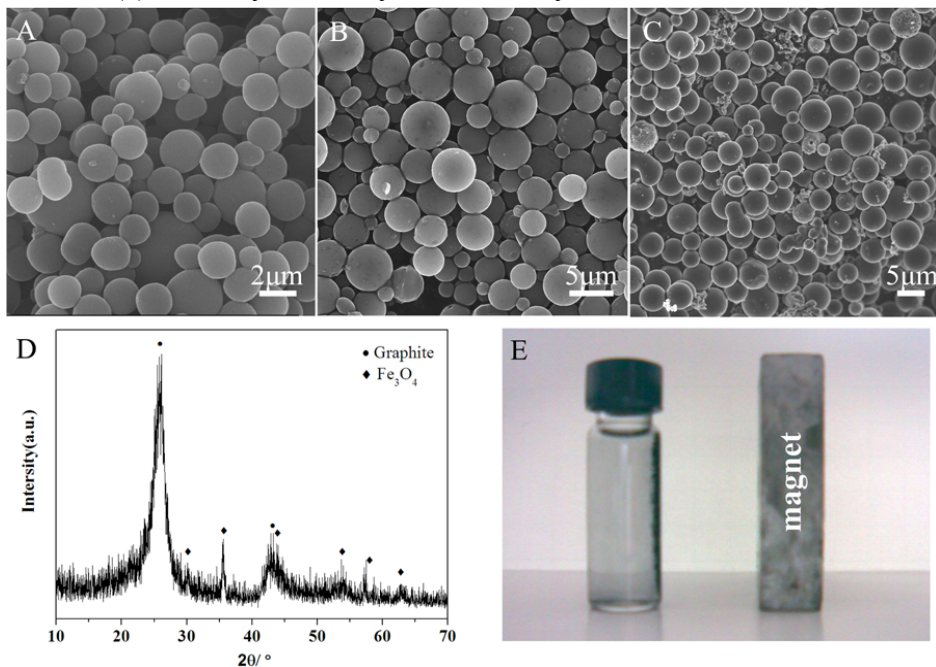


**Fig. S5** Typical TEM images of MGCSs prepared with different saccharides: (A) sucrose, (B) fructose, and (C) starch; (D) XRD patterns of MGCSs prepared with sucrose; (E) image of magnetic response of MGCSs prepared with sucrose and ferrous gluconate.

**Table S1** Adsorption capacity of MGCSs for RhB in different cycles.

Number of cycling	1	2	3	4	5	6	7	8	9	10
Adsorption quantity (mg g <sup>-1</sup> )	73.80	73.09	72.15	67.79	62.97	61.91	61.20	60.62	60.50	60.73

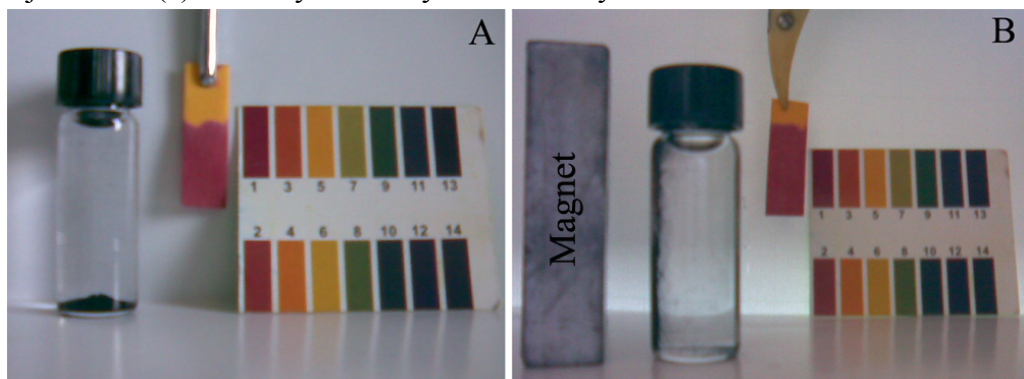


**Fig. S6** Image of magnetic response of MGCSs in acidity solution of pH = 1, (A) before a week; (B) dipping for a week.

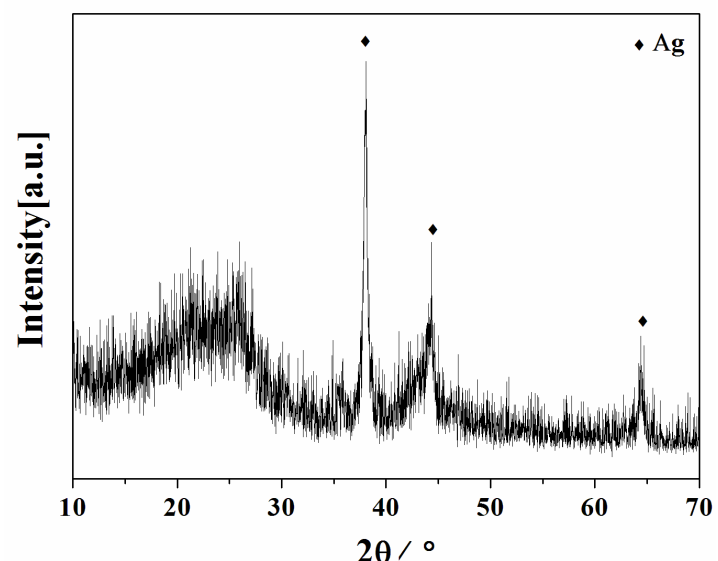


**Fig. S7** XRD patterns of MGCS@Ag microspheres.

**Table S2** Phosphopeptides ion peaks observed in the MALDI Mass Spectrum of tryptic digest of  $\alpha$ -casein and  $\beta$ -casein.

NO.	phosphopeptide sequences	Number of phosphorylation sites	[M+H] <sup>+</sup>
$\alpha 1$	TVDME[pS]TEVF	1	1237.17
$\alpha 2$	TVDME[pS]TEVFTK	1	1467.17
$\alpha 3$	EQLSPT[pS]EENSKK	1	1539.10
$\alpha 4$	EQL[pS]T[pS]EENSKK	2	1561.54*
$\alpha 5$	TVDME[pS]TEVFTKK	1	1595.16
$\alpha 6$	VPQLEIVPN[pS]AEER	1	1660.28
$\alpha 7$	YKVPQLEIVPN[pS]AEER	1	1833.20
$\alpha 8$	DIG[pS]E[pS]TEDQAMETIK	2	1927.92
$\alpha 9$	YKVPQLEIVPN[pS]AEER	1	1952.19
$\alpha 10$	NTMEHV[pS] [pS] [pS]EESII[pS]QETYKQ	4	2617.88
$\alpha 11$	LRLKKYKVPQLEIVPN[pS]AEERL	1	2704.10
$\alpha 12$	QMEAE[pS]I[pS][pS][pS]EEIVPNPNP[pS]VEQK	5	2721.21
$\alpha 13$	NTMEHV[pS][pS][pS]EE[pS]SQETYKQ	4	2746.71
$\alpha 14$	KEKVNEL[pS]KDIG[pS]E[pS]TEDQAMEDIKQ	3	2934.92
$\alpha 15$	NANEEEYSIG[pS][pS][pS]EE[pS]AEVATEEVK	4	3008.40
$\beta 1$	FQ[pS]EEQQQTEDELQDK	1	2061.48
$\beta 2$	FQ[pS]EEQQQTEDELQDKIHPF	1	2556.67
$\beta 3$	RELEELNVPGEIVE[pS]L[pS][pS][pS]EESITR	4	3122.55

\*[M+Na]<sup>+</sup>